

Radiation-defect-perturbed  $\text{Er}^{3+}$  and  $\text{Mn}^{2+}$  optical transitions in  $\text{RbMgF}_3$ 

D. K. Sardar, M. D. Shinn, and W. A. Sibley

*Department of Physics, Oklahoma State University, Stillwater, Oklahoma 74078*

(Received 2 February 1982; revised manuscript received 4 June 1982)

The optical properties of defect-perturbed  $\text{Er}^{3+}$  and  $\text{Mn}^{2+}$  ions in  $\text{RbMgF}_3$  crystals have been investigated. Previous research has shown that  $\text{Mn}^{2+}$  optical transitions can be enhanced by as much as  $10^5$  through spin coupling with a nearby  $F$  center. This result has been further verified. Evidence is presented that radiation-defect- $\text{Er}^{3+}$  complexes can be formed in  $\text{RbMgF}_3$ . Both the perturbed  $\text{Mn}^{2+}$  and  $\text{Er}^{3+}$  have detectable optical transitions. Our analysis suggests that, although the perturbed  $\text{Er}^{3+}$  transitions are shifted in energy, the oscillator strength of the  $\text{Er}^{3+}$   ${}^4S_{3/2} \rightarrow {}^4I_{15/2}$  transition is increased by at most an order of magnitude by the presence of  $F$  centers. The  ${}^4S_{3/2} \rightarrow {}^4I_{15/2}$  transition for the radiation-defect-perturbed  $\text{Er}^{3+}$  persists to room temperature and has a lifetime of 210  $\mu\text{s}$ .

## I. INTRODUCTION

The physical properties of materials can be substantially modified by the presence of impurity ions and/or radiation-induced defects. Although the optical properties of impurities and radiation defects have been extensively studied in the past, there are a number of fluoride crystals, such as  $\text{RbMgF}_3$ , with potential as laser hosts that require more detailed investigation. The transparent "window" for  $\text{RbMgF}_3$  ranges from 140 nm to 6  $\mu\text{m}$ . Moreover, in  $\text{RbMgF}_3$  radiation-induced  $F$  centers are immobile even at 300 K. Thus,  $F$ -center aggregation does not occur during irradiation at room temperature. Careful annealing of these crystals results in aggregation of the defects and the possibility of studying defect interactions.

The properties of  $\text{Er}^{3+}$  have been studied in detail for a number of fluorides.<sup>1-11</sup> We report in this paper the effects of electron irradiation on nominally pure  $\text{Er}^{3+}$ - and  $\text{Er}^{3+}$ - $\text{Mn}^{2+}$ -doped  $\text{RbMgF}_3$  crystals. Previously, the effects of irradiation and thermal annealing on pure and  $\text{Mn}^{2+}$ -doped  $\text{RbMgF}_3$  crystals were studied.<sup>12-14</sup> The present investigation confirms and extends the previous results for  $\text{Mn}^{2+}$ -doped crystals which showed that the oscillator strength of  $\text{Mn}^{2+}$  transitions can be drastically enhanced due to the presence of radiation-induced  $F$ -center defects.<sup>15-20</sup> The emission and excitation spectra for defect-perturbed  $\text{Mn}^{2+}$  transitions are easily observed due to the enhancement of the oscillator strength.

In the  $\text{RbMgF}_3$  lattice  $\text{Mn}^{2+}$  and  $\text{Er}^{3+}$  impurity ions substitutionally replace  $\text{Mg}^{2+}$  ions. The six  $\text{Mg}^{2+}$  ions in a unit cell are in sites of  $C_{3v}$  symmetry. However, two of these ions have equidistant

ligands approximating local  $O_h$  symmetry (site 1). The other four  $\text{Mg}^{2+}$  ions are in more constricted sites with the ligands at nonequidistant points (site 2). Charge compensation for divalent  $\text{Mn}^{2+}$  ions is not required, whereas in the case of trivalent  $\text{Er}^{3+}$  ions charge compensation could be accomplished either by fluorine interstitials or by monovalent  $\text{Rb}^+$  vacancies.<sup>11</sup>

## II. MATERIALS AND EXPERIMENTAL TECHNIQUES

The single crystals investigated in this work were grown by J. J. Martin at the Oklahoma State University Crystal Growth Laboratory. The crystal growth melts for the doped samples contained 1 at. % of  $\text{Er}^{3+}$  and/or 1 at. % of  $\text{Mn}^{2+}$ . The impurity concentrations in the crystals varied greatly with position. If an oscillator strength of  $f = 10^{-6}$  is assumed for the  $\text{Er}^{3+}$   ${}^2H_{11/2}$  optical transition<sup>1</sup> (520 nm), the  $\text{Er}^{3+}$  concentration could be calculated from optical absorption data taken on a Cary-14 spectrophotometer. In order to obtain the necessary high sensitivity in these measurements because of the low oscillator strengths, a 0–0.1 O.D. slidewire was used in the Cary-14. In all cases, the measured  $\text{Er}^{3+}$  concentration was more than an order of magnitude less than the 1 at. % added to the growth melts.

Low-temperature measurements were made with the crystals in a CTI cryogenic cooler which had a resistance heater for temperature control between 12 and 300 K. In this particular work, two detectors were used to cover the wide range of emission spectra. A cooled RCA 31034 photomultiplier tube

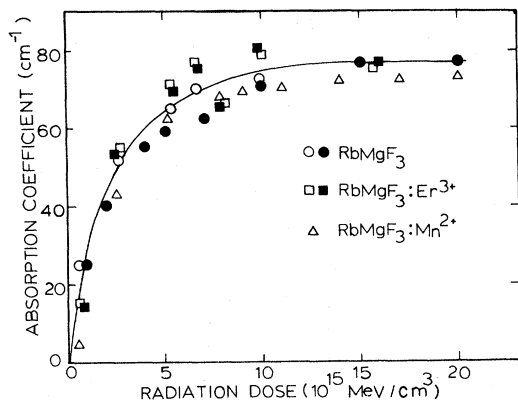


FIG. 1.  $F$ -center absorption as a function of absorbed radiation energy for undoped (circles),  $\text{Er}^{3+}$ -doped (squares), and  $\text{Mn}^{2+}$ -doped (triangles)  $\text{RbMgF}_3$  crystals irradiated at 300 K.

(PMT) for the visible range and an RCA 7102 PMT cooled at dry ice for the near-infrared region were utilized. Emission spectra were measured on a 0.8-m Spex monochromator and excitation spectra were taken using a 0.22-m Spex monochromator. The exciting light from a 75-W Xe lamp was chopped at the desired frequency. The intensity of the exciting light from the Xe lamp and minimate monochromator was measured with a Spectra Radiometer Model 301. The excitation spectra were corrected accordingly. Lifetime measurements were accomplished with a Biomation Model 610B connected to a Nicolet 1070 signal averager.

The samples were irradiated at 300 K with 1.5-MeV electrons at a current of about  $0.1 \mu\text{A}/\text{cm}^2$  in the Oklahoma State University Van de Graaff facility. The electron irradiation intensity in air was measured using a Ag-glass dosimeter and found to be about  $2.2 \times 10^{13} \text{ MeV cm}^{-3} \text{ s}^{-1}$ . For thermal-

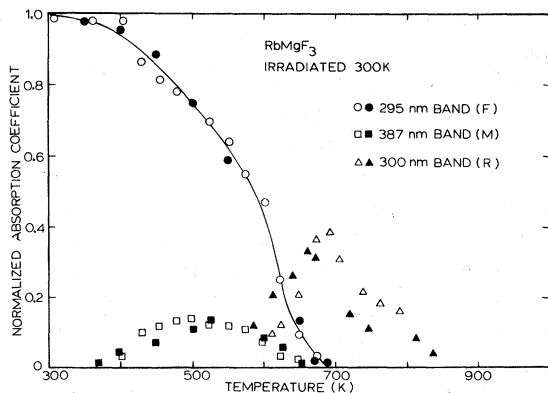


FIG. 2. Normalized thermal-annealing data for undoped  $\text{RbMgF}_3$  crystals irradiated at 300 K with 1.5-MeV electrons for 15 min.

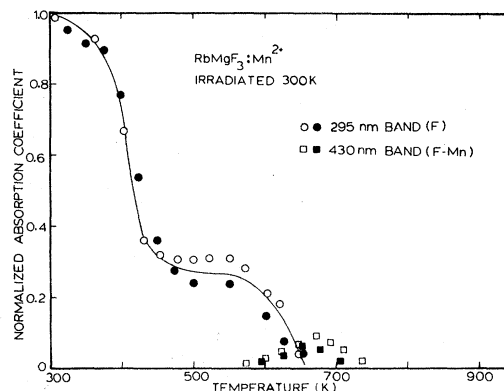


FIG. 3. Normalized thermal-annealing data for  $\text{RbMgF}_3:\text{Mn}^{2+}$  samples after electron irradiation at 300 K with 1.5-MeV electrons for 15 min.

annealing experiments the samples were held at desired temperatures in the furnace for 10 min and then cooled to room temperature.

### III. RESULTS

#### A. Irradiation and annealing experiments

When nominally pure  $\text{Er}^{3+}$ - and/or  $\text{Mn}^{2+}$ -doped  $\text{RbMgF}_3$  crystals are irradiated with electrons at room temperature, stable  $F$ -center defects are formed. The absorption band due to  $F$  centers occurs around 300 nm, and the polarized absorption spectrum was studied previously.<sup>14</sup> The growth of  $F$  centers as a function of radiation dose is portrayed in Fig. 1. No noticeable difference in the production of stable  $F$  centers in doped and undoped samples is observed. The concentration of  $F$  centers can be obtained from the expression  $fN = 7.3 \times 10^{15} \alpha_m W \text{ cm}^{-3}$ , where  $f$  is the oscillator strength,  $N$  is the concentration,  $\alpha_m$  is the maximum absorption coefficient, and  $W$  is the halfwidth of the band. From this expression, using  $f = 0.5$  and  $W = 0.95 \text{ eV}$ , the  $F$ -center concentration at a radiation dose of  $10^{16} \text{ MeV}/\text{cm}^3$  is calculated to be about  $10^{18} \text{ cm}^{-3}$ .

Previous observations of  $\text{RbMgF}_3$  indicated that  $F$  centers do not aggregate under irradiation at room temperature<sup>12,14</sup>; however, at higher temperatures  $F$  centers do move to form complexes. Figure 2 illustrates the effect of annealing. The  $F$  centers aggregate to form  $F_2(M)$  and  $F_3(R)$  centers at different annealing temperatures in nominally pure samples. The  $F_2$ -center absorption peaks at about 387 nm, and  $F_3$ -center absorption peaks at about 300 nm.<sup>14</sup> In the process of formation of defect

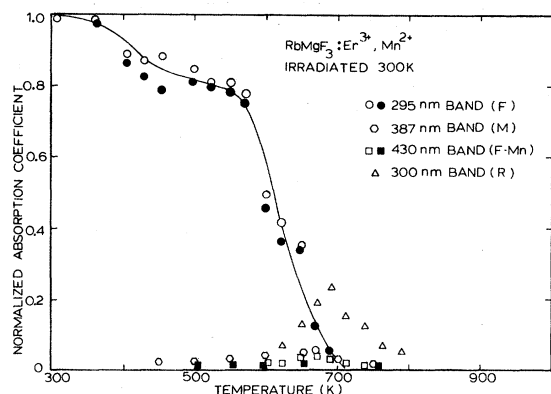


FIG. 4. Normalized thermal-annealing data for  $\text{RbMgF}_3:\text{Er}^{3+}, \text{Mn}^{2+}$  crystals after electron irradiation at 300 K with 1.5-MeV electrons for 15 min.

complexes, the total  $F$ -center concentration is conserved within 90% of its initial value for annealing temperatures up to 650 K. Figure 3 depicts the annealing behavior of  $F$  centers in crystals doped with  $\text{Mn}^{2+}$  ions. Two types of defect complexes of  $F$ - $\text{Mn}^{2+}$  ions are formed. These defects have absorption bands at 430 and 700 nm (site-2 ions), and 420 and 600 nm (site-1 ions). Emission from  $F_2$  and  $F_3$  centers was also observed in the  $\text{Mn}^{2+}$ -doped samples at about the same annealing temperature regimes as the pure samples, but the intensity of these bands was much smaller than that due to  $F$ - $\text{Mn}^{2+}$  defects.

The sharp decrease in  $F$ -center concentration at 400 K in Fig. 3 occurs because fluorine interstitials trapped by  $\text{Mn}^{2+}$  ions during irradiation are released at this temperature and annihilate  $F$  centers.<sup>13</sup> After the initial reduction of  $F$  centers at 400 K, the annealing process follows almost the same pattern as that observed for undoped samples. These results agree very well with those obtained by Koumvakalis and Sibley.<sup>12</sup> Figure 4 portrays the effect of annealing of  $F$  centers and the formation of defect complexes in a  $\text{RbMgF}_3:\text{Er}^{3+}$  crystals

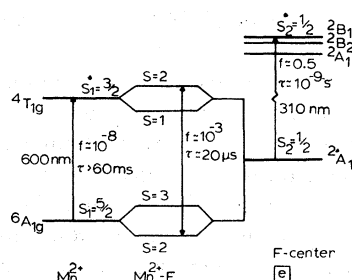


FIG. 5. Schematic diagram for spin coupling between the ground and first excited states of isolated  $\text{Mn}^{2+}$  and  $F$  center.

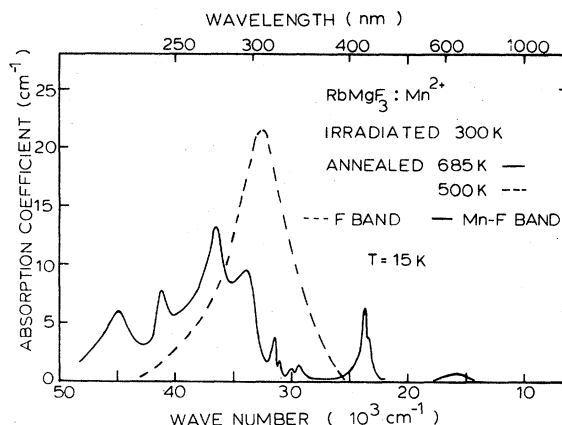


FIG. 6. Absorption spectrum of  $F$  center (dashed line) at 300 K, and absorption spectrum of  $\text{Mn-F}$  band at 15 K.

which inadvertently contained about (20–100)-ppm  $\text{Mn}^{2+}$  ions. After the initial small drop of  $F$  centers, due to the presence of unintentionally added  $\text{Mn}^{2+}$  ions, the annealing process essentially follows the same pattern as that for undoped samples. It appears that the high concentration of  $\text{Er}^{3+}$  ions in the  $\text{RbMgF}_3:\text{Er}^{3+}$  crystal has little influence on the annealing process.

#### B. Emission and excitation for $\text{Mn}^{2+}$ - $F$ complexes

As mentioned earlier, the oscillator strengths of originally forbidden transitions of  $\text{Mn}^{2+}$  ions are enhanced when radiation-induced  $F$  centers are present as first nearest neighbors. In Fig. 5 the energy levels for the ground and first excited states of isolated  $\text{Mn}^{2+}$  ions and  $F$  centers are portrayed schematically. The transition between the ground state  ${}^6A_{1g}$  and the first excited state  ${}^4T_{1g}$  of  $\text{Mn}^{2+}$  ions in  $O_h$  symmetry is forbidden by both symmetry and spin. This transition has a lifetime  $\tau > 60$  ms and an oscillator strength  $f \sim 10^{-8}$ .<sup>19</sup> On the other hand, the transition for  $F$  centers is both symmetry and spin allowed. As the electrons of  $\text{Mn}^{2+}$  ions couple with those of  $F$  centers, the transition between the excited and ground states for the  $\text{Mn}^{2+}$ - $F$  complexes becomes spin allowed as portrayed in Fig. 5. As  $F$  centers couple with  $\text{Mn}^{2+}$  ions, the  $F$  band essentially disappears. Since the oscillator strengths of the  $F$  centers and  $\text{Mn}^{2+}$  ions must be conserved, the  $\text{Mn}^{2+}$  transitions are enhanced. Figure 6 illustrates that the area under the  $F$  band after annealing at 500 K (dashed line) is about equal to the area under the  $\text{Mn}^{2+}$ - $F$  center absorption after annealing at 685 K (solid line). This suggests that the oscillator strength is conserved. The  $\text{Mn}^{2+}$ - $F$

TABLE I. Absorption and emission bands of  $\text{Mn}^{2+}$  in different sites.

	Irradiated				Irradiated and annealed	
	Site 1		Site 2		Perturbed spectrum	
	( $\text{cm}^{-1}$ )	(nm)	( $\text{cm}^{-1}$ )	(nm)	( $\text{cm}^{-1}$ )	(nm)
<b>Absorption</b>						
${}^6A_1 \rightarrow {}^4E, {}^4A_1$	23 810	420	23 256	430	24 390	410
${}^6A_1 \rightarrow {}^4T_1$	16 667	600	14 286	700	14 286	700
<b>Emission</b>						
${}^4T_1 \rightarrow {}^6A_1$	14 085	710	11 494	870	11 494	870

center transitions between 250 and 320 nm are much enhanced compared to the same  $\text{Mn}^{2+}$  transitions in  $\text{RbMnF}_3$ .

Since there are two different types of symmetry sites for  $\text{Mn}^{2+}$  ions in the crystal lattice, two distinctly different emission and excitation spectra from such sites are observed. The energies of the absorption and emission bands associated with these sites are shown in Table I. These spectra are depicted in Figs. 7 and 8. Figure 7 shows a 710-nm emission band (depicted as a dashed line) and its excitation spectrum (solid line) with peaks at 420 and 600 nm. Figure 8 portrays an 870-nm emission band and its excitation spectrum with peaks at 430 and 700 nm. Lifetimes ( $\tau$ ) measured for both transitions are found to be about 20  $\mu\text{s}$ . This is consistent with an oscillator strength of  $\sim 10^{-3}$ . This value for the oscillator strength is in agreement with the previous data.<sup>12,13</sup>

Figure 9 illustrates the variation of intensities of absorption and excitation spectra for the 420 and 430-nm  $\text{Mn}^{2+}$ - $F$  bands with annealing temperature. The intensities of both the excitation and absorption

increase in the same manner until 700 K after which both drop drastically. From previous work, it was determined that the approximate oscillator strength of the perturbed  $\text{Mn}^{2+}$ - $F$  center absorption at 430 nm was 0.05.<sup>13</sup> Thus the concentration of irradiation-produced *statistical* pairs ( $F$  centers immobile) at 300 K can be determined from the expression  $fN_{\text{Mn-F}} = 7.3 \times 10^{15} \alpha_m W \text{ cm}^{-3}$ . From experiment,  $\alpha_m = 0.27 \text{ cm}^{-1}$  and  $W = 0.14 \text{ eV}$ , so  $N_{\text{Mn-F}} \approx 6 \times 10^{15} \text{ cm}^{-3}$ . Of course, if the  $F$ -center and  $\text{Mn}^{2+}$ -impurity concentrations are known, it is possible to calculate the expected concentration of irradiation-produced pairs. The  $F$ -center concentration determined from available information, e.g.,  $f = 0.5$ ,  $\alpha_m = 76 \text{ cm}^{-1}$ , and  $W = 0.95 \text{ eV}$ , is  $N_F = 1.1 \times 10^{18} \text{ cm}^{-3}$ . Since 1 at. % of  $\text{Mn}^{2+}$  was added to the melt in crystal growth and only about 10% enters the crystal,  $N_{\text{Mn}} \approx 10^{19} \text{ cm}^{-3}$ . Therefore, from strictly statistical considerations  $N_{\text{Mn-F}} = (6/N_0)N_F N_{\text{Mn}} \approx 6 \times 10^{15} \text{ cm}^{-3}$ , where  $N_0 = 1.24 \times 10^{22} \text{ cm}^{-3}$ . The exact agreement is clearly fortuitous. Nonetheless, it appears that statistical defect production does occur and there are

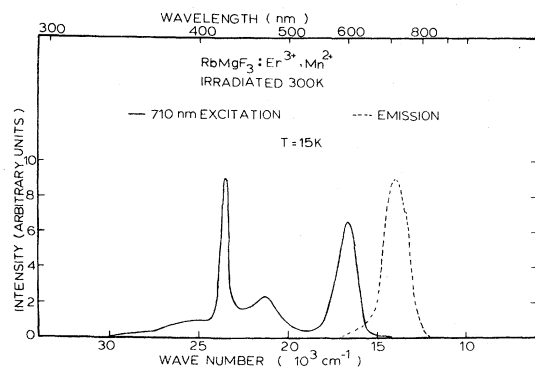


FIG. 7. 710-nm emission band (dashed line) at 15 K from a  $\text{RbMgF}_3:\text{Er}^{3+},\text{Mn}^{2+}$  crystal irradiated with 1.5-MeV electrons at 300 K and annealed to 500 K, and its excitation spectrum (solid line).

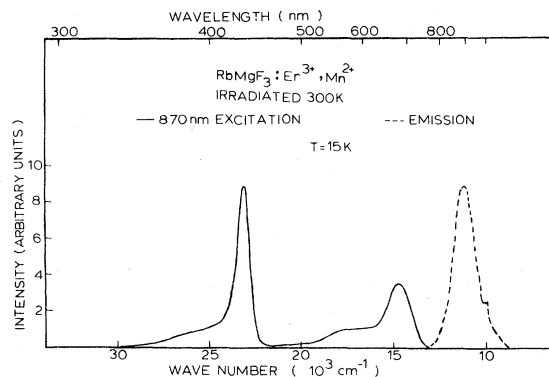


FIG. 8. Excitation spectrum (solid line) of an 870-nm emission band (dashed line) at 15 K from  $\text{RbMgF}_3:\text{Er}^{3+},\text{Mn}^{2+}$  crystal irradiated with 1.5-MeV electrons at 300 K and annealed to 500 K.

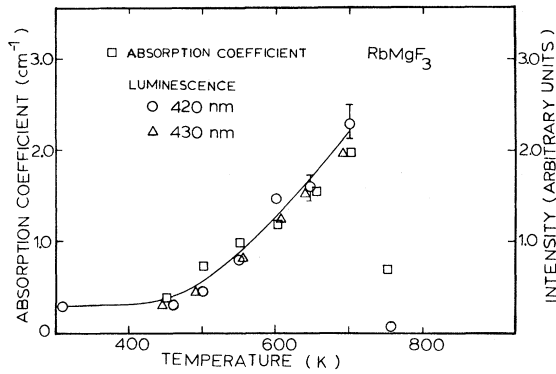


FIG. 9. Absorption coefficient and excitation intensity of 420- and 430-nm  $\text{Er}^{3+}:\text{Mn}^{2+}$  crystals.

no preferred defect production sites.

An analysis of the annealing data shown in Fig. 3 suggests that only about  $2 \times 10^{17} \text{ cm}^{-3}$   $F$  centers are available around 500 K to move to  $\text{Mn}^{2+}$  ions. This places an upper limit on the number of  $\text{Mn}^{2+}-F$  center pairs expected. The concentration achieved at 700 K was  $6 \times 10^{16} \text{ cm}^{-3}$  in each type of site for a total of  $\sim 10^{17} \text{ cm}^{-3}$  defect pairs.

### C. Emission of perturbed $\text{Er}^{3+}$ ions

In the preceding paper,<sup>11</sup> detailed absorption and emission spectra for  $\text{Er}^{3+}$  ions in  $\text{RbMgF}_3$  and in  $\text{RbMgF}_3:\text{Mn}$  crystals were reported. In this previous work, it was found that when both  $\text{Mn}^{2+}$  and  $\text{Er}^{3+}$  ions are present in  $\text{RbMgF}_3$  two sets of spectra are observed. These sets, denoted as  $a$  and  $b$ , are illustrated in Fig. 10. The solid line in Fig. 10

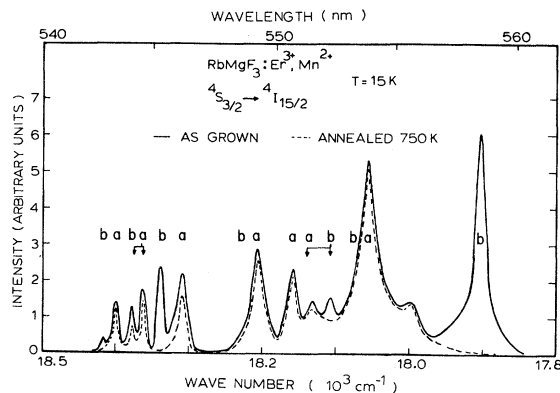


FIG. 10. Emission spectrum of  ${}^4S_{3/2} \rightarrow {}^4I_{15/2}$  at 15 K (solid line) for  $\text{Er}^{3+}$  in  $\text{RbMgF}_3:\text{Er}^{3+},\text{Mn}^{2+}$  crystal "as grown," and excitation with 520-nm light, and emission for the same transition in annealed sample (dashed line). The letters above the emission bands are explained in the text.

TABLE II.  ${}^4S_{3/2} \rightarrow {}^4I_{15/2}$  emission lines from  $\text{Er}^{3+}$  ions in different sites.

Site 1 <i>a</i> ( $\text{cm}^{-1}$ )	Perturbed spectrum (irradiated and annealed) ( $\text{cm}^{-1}$ )	Site 2 <i>b</i> ( $\text{cm}^{-1}$ )
18 400		18 415
18 376	18 352	18 379
18 363	18 335	18 337
18 313	18 278	18 232
18 202	18 177	18 140
18 158	18 132	18 101
18 124	18 097	18 067
18 056	18 031	17 907

shows the emission from the  ${}^4S_{3/2} \rightarrow {}^4I_{15/2}$  for the  $\text{Er}^{3+}$  in "as-grown" specimens, and the dashed line shows the same transition in an annealed sample (750 K). The energies of the lines associated with the  ${}^4S_{3/2} \rightarrow {}^4I_{15/2}$  transitions for the two sites are given in Table II. These transitions are parity forbidden. The lifetime at 7 K of the transitions labeled  $a$  is  $\sim 175 \mu\text{s}$  and the transitions labeled  $b$  show a double lifetime of 320 and 80  $\mu\text{s}$ .

The  $\text{Er}^{3+}$  spectra in  $\text{RbMgF}_3:\text{Mn}^{2+},\text{Er}^{3+}$  are not changed by irradiation at 300 K. This is expected since  $F$  centers are not mobile at 300 K. However, when irradiated  $\text{RbMgF}_3:\text{Er}^{3+},\text{Mn}^{2+}$  crystals are annealed at 450 K, a new emission ( ${}^4S_{3/2} \rightarrow {}^4I_{15/2}$ ), shown in Fig. 11, is observed. The relative intensity scales of Figs. 10 and 11 are normalized. One question that must be asked is, Are these new lines really due to  $\text{Er}^{3+}$  ions associated with  $F$  centers? In order to answer this question, an unirradiated  $\text{RbMgF}_3:\text{Er}^{3+},\text{Mn}^{2+}$  crystal was heat treated to 450 K and quenched. In this instance, the transitions

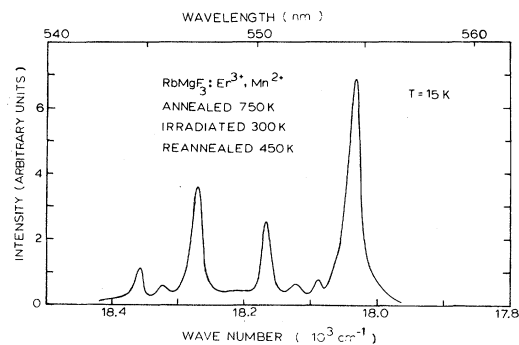


FIG. 11. Perturbed emission spectrum  ${}^4S_{3/2} \rightarrow {}^4I_{15/2}$  at 15 K from  $\text{RbMgF}_3:\text{Er}^{3+},\text{Mn}^{2+}$  crystal irradiated at 300 K with 1.5-MeV electron for 15 min and annealed to 450 K.

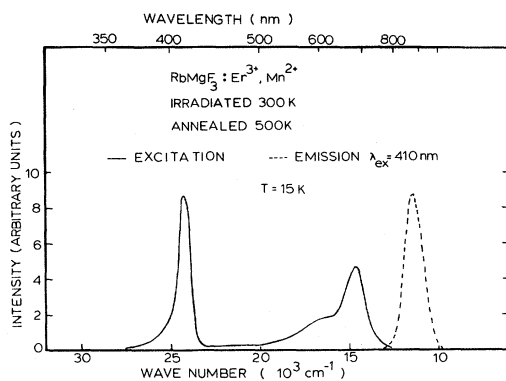


FIG. 12. Emission band (dashed line) at 15 K from  $\text{RbMgF}_3:\text{Er}^{3+}, \text{Mn}^{2+}$  crystal irradiated with 1.5-MeV electrons at 300 K, annealed to 500 K, and excited at 410-nm band shown in excitation spectrum (solid line).

labeled *b* in Fig. 10 decreased, but no new lines were observed. Then a  $\text{RbMgF}_3:\text{Er}^{3+}$  was irradiated and annealed. The new lines were not observed. It should be mentioned that annealing a  $\text{RbMgF}_3$  crystal (either irradiated or unirradiated) that contains both  $\text{Mn}^{2+}$  and  $\text{Er}^{3+}$  at 750 K eliminates the transitions labeled *b* in Fig. 10. It appears from the above experiments that both  $\text{Mn}^{2+}$  impurities and *F* centers are necessary to produce the spectrum shown in Fig. 11.

Further evidence supporting the supposition that  $\text{Mn}^{2+}$  is involved in producing the spectrum in Fig. 11 is that when the perturbed  $\text{Er}^{3+}$  spectrum appears (tabulated in Table II), a third perturbed  $\text{Mn}^{2+}$  spectrum (illustrated in Fig. 12 and tabulated in Table I) is also present. The intensity scale in Fig. 12 is normalized to those in Figs. 7 and 8. This spectrum is slightly different to that shown in Fig. 8, but the  $\text{Mn}^{2+}$  is most likely in the same site with a different perturbation. The intensity of the excitation peak at 410 nm is at least 5 times weaker than that of the 430-nm peak.

#### IV. DISCUSSION

The primary purpose of this research was to determine if the oscillator strength of  $\text{Er}^{3+}$  transitions are changed appreciably by the presence of perturbing defects. Oscillator strength changes could occur from wave-function mixing of the  $\text{Er}^{3+}$  4*f* wave function with ligand wave functions. This mixing is small for  $\text{Er}^{3+}$  because of shielding by 5*s* and 5*p* electrons. Since *F* centers have very extended wave functions, more intimate mixing might occur and a large oscillator strength change

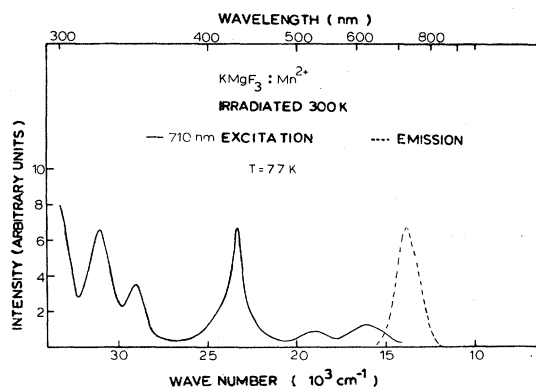


FIG. 13. 710-nm emission band (dashed line) from  $\text{KMgF}_3:\text{Mn}^{2+}$  crystal irradiated with 1.5-MeV electrons at 300 K, and its excitation spectrum (solid line) at 77 K.

could exist. The question, What is the magnitude of the  $\text{Er}^{3+}$  oscillator strength increase due to the presence of *F* centers? is a crucial one.

In order to answer the question asked above, it is necessary to identify the  $\text{Mn}^{2+}$  and  $\text{Er}^{3+}$  sites responsible for the emission in Figs. 7, 8, 10, 11, and 12. As mentioned earlier, the  $\text{Mn}^{2+}$  ions can substitute for  $\text{Mg}^{2+}$  ions in  $C_{3v}$  sites with equally or unequally spaced ligands. Previous work on  $\text{KMgF}_3:\text{Mn}^{2+}$  yielded spectra for  $\text{Mn}^{2+}$  ions in sites with equally spaced ligands.<sup>15,16</sup> The spectrum for  $\text{Mn}^{2+}$ -*F* center complexes in  $\text{KMgF}_3:\text{Mn}^{2+}$  is shown in Fig. 13. Notice that the emission energy is the same as that shown in Fig. 7 for  $\text{RbMgF}_3:\text{Mn}^{2+}, \text{Er}^{3+}$ . Thus, it appears that the 710-nm emission depicted in Fig. 7 is from  $\text{Mn}^{2+}$ -*F*-center defects in which the  $\text{Mn}^{2+}$  ions replaced  $\text{Mg}^{2+}$  ions in the sites with equidistant ligands (site 1). This suggests that the emission spectra shown in Figs. 8 and 12 arise from complexes in which the  $\text{Mn}^{2+}$  ions are in the more constricted  $C_{3v}$  sites (site 2). Further evidence for this assignment comes from the crystal-field calculations of Tanabe and Sugano.<sup>21,22</sup> Greater ligand pressure shifts the emission and absorption to longer wavelength. Therefore, we conclude that the 710-nm emission is from  $\text{Mn}^{2+}$  ions in site 1 and the 870-nm emission is from  $\text{Mn}^{2+}$  in site 2. Since the  $\text{Mn}^{2+}$ -*F*-center defect responsible for the emission shown in Fig. 12 is present concurrently with the perturbed  $\text{Er}^{3+}$  emission shown in Fig. 11, it is necessary to determine the  $\text{Er}^{3+}$  sites responsible for the spectra in Figs. 10 and 11 to state the defect configuration.

In the preceding paper,<sup>11</sup> it was determined that spectrum *a* in Fig. 10 arises from  $\text{Er}^{3+}$  in site 1 and

the *b* spectrum comes from  $\text{Er}^{3+}$  ions in site 2. The radiation-induced  $\text{Er}^{3+}$  spectrum is a rigid energy shift of about  $-25 \text{ cm}^{-1}$  of the *a* spectrum. This suggests the radiation-induced  $\text{Er}^{3+}$  spectrum is from a complex consisting of an *F* center between a  $\text{Mn}^{2+}$  ion in site 2 and an  $\text{Er}^{3+}$  ion in site 1.

Although the absorption spectra for irradiated  $\text{RbMgF}_3:\text{Mn}^{2+}$  and  $\text{KMgF}_3:\text{Mn}^{2+}$  are similar, the excitation spectra between 250 and 400 nm are not, as can be seen through a comparison of Figs. 7 and 13. The excitation spectra differ because of an intense 420-nm emission from the  $\text{Mn}^{2+}$  in  $\text{RbMgF}_3$  which strongly reduces the nonradiative transitions to lower energy levels.

Perhaps the best method of comparing oscillator strengths of *F*-center-perturbed  $\text{Er}^{3+}$  ions and those without *F*-center neighbors is to evaluate the lifetimes. The lifetime for the transitions in Fig. 11 at 15 K is 320  $\mu\text{s}$ . Through the courtesy of Dr. R. C. Powell's group, the lifetime of the perturbed  $\text{Er}^{3+}$  transitions was remeasured at 12 K using suitable dye-laser excitation and a boxcar integrator. The lifetime was 300–350  $\mu\text{s}$ . No fast component of lifetime shorter than 100  $\mu\text{s}$  was observed. At 300 K the lifetime was 210  $\mu\text{s}$ . If the measured lifetime at 15 K for defect-perturbed  $\text{Er}^{3+}$  is the radiative lifetime, then it corresponds to an oscillator strength of about  $10^{-6}$  for the  $^4S_{3/2} \rightarrow ^4I_{15/2}$  transition. An oscillator strength of  $10^{-7}$  has been reported for this transition in  $\text{LaF}_3:\text{Er}^{3+}$ .<sup>1</sup> The radiative lifetime for the unperturbed  $\text{Er}^{3+}$   $^4S_{3/2} \rightarrow ^4I_{15/2}$  transition is about 1 ms.<sup>1</sup> Thus it appears that the *F* center enhances the  $\text{Er}^{3+}$  oscillator strength by, at most, an order of magnitude in  $\text{RbMgF}_3$ .

## V. SUMMARY

We note the following:

(1) Two different lattice sites with  $C_{3v}$  symmetry, one with essentially equidistant ligands, are available to  $\text{Mn}^{2+}$  or  $\text{Er}^{3+}$  impurity ions substituting for  $\text{Mg}^{2+}$  ions. The  $\text{Mn}^{2+}$ –*F*-center pairs and  $\text{Er}^{3+}$  ions in both sites are observed optically.

(2) Oscillator strength enhancement of  $10^5$  for  $\text{Mn}^{2+}$  ions due to the presence of *F* centers has been further verified.

(3) Since *F* centers are not mobile in  $\text{RbMgF}_3$  at 300 K, only *statistical* production of radiation defect-impurity pairs is observed at this temperature.

(4) In  $\text{RbMgF}_3$  crystals containing both  $\text{Mn}^{2+}$  and  $\text{Er}^{3+}$  impurities, a perturbed  $\text{Er}^{3+}$  spectrum is observed after irradiation and heat treatment. A new perturbed  $\text{Mn}^{2+}$  spectrum is also concurrently observed. Analysis suggests this  $\text{Er}^{3+}$   $^4S_{3/2} \rightarrow ^4I_{15/2}$  optical transition is enhanced by an order of magnitude due to the presence of *F* centers.

(5) All observable radiation defect spectra are annealed at 750 K.

## ACKNOWLEDGMENTS

The authors would like to thank Professor Z. Al-Shaieb for his help in orienting the crystals. Several discussions with Professor R. Orbach were extremely helpful and we express our deep appreciation to him. We also thank Professor R. C. Powell for helpful discussions. The work was supported by NSF-DMR Grant No. 8105017.

<sup>1</sup>M. J. Weber, Phys. Rev. **157**, 262 (1967).

<sup>2</sup>J. M. Flaherty and B. DiBartolo, J. Lumin. **8**, 51 (1973).

<sup>3</sup>B. A. Wilson, W. M. Yen, J. Hagerty, and G. F. Imbush, Phys. Rev. B **19**, 4238 (1979).

<sup>4</sup>M. R. Brown, K. G. Roots, and W. A. Shand, J. Phys. C **2**, 593 (1969).

<sup>5</sup>M. V. Petrov and A. M. Tkachuk, Opt. Spektrosk. (USSR) **45**, 147 (1978).

<sup>6</sup>H. P. Christensen, Phys. Rev. B **19**, 6564 (1979).

<sup>7</sup>D. S. Moore and J. C. Wright, J. Chem. Phys. **74**, 1626 (1981).

<sup>8</sup>G. M. Renfro, J. C. Windscheif, W. A. Sibley, and R. F. Belt, J. Lumin. **22**, 51 (1980).

<sup>9</sup>I. V. Mochalov, Phys. Status Solidi A **55**, 79 (1979).

<sup>10</sup>T. C. Ensign and N. E. Byer, Phys. Rev. B **6**, 3227 (1972).

<sup>11</sup>M. D. Shinn, J. C. Windscheif, D. K. Sardar, and W.

A. Sibley, preceding paper, Phys. Rev. B **26**, 2371 (1982).

<sup>12</sup>N. Koumvakalis and W. A. Sibley, Phys. Rev. B **13**, 4509 (1976).

<sup>13</sup>W. A. Sibley and N. Koumvakalis, Phys. Rev. B **14**, 35 (1976).

<sup>14</sup>A. Podinsh and W. A. Sibley, Phys. Rev. B **18**, 5921 (1978).

<sup>15</sup>K. H. Lee and W. A. Sibley, Phys. Rev. B **12**, 3392 (1975).

<sup>16</sup>S. I. Yun, K. H. Lee, W. A. Sibley, and W. E. Vehse, Phys. Rev. B **10**, 1665 (1974).

<sup>17</sup>J. Ferguson, in *Progress in Inorganic Chemistry*, edited by S. J. Lippard (Interscience, New York, 1970), Vol. 12, p. 159.

<sup>18</sup>J. Ferguson, E. R. Krausz, and J. G. Guggenheim, Mol. Phys. **27**, 577 (1974).

<sup>19</sup>J. Ferguson, J. G. Guggenheim, and Y. Tanabe, J. Appl. Phys. **36**, 1046 (1965).

<sup>20</sup>M. S. Young, E. E. Kohnke, and L. E. Halliburton, Bull. Am. Phys. Soc. **20**, 328 (1975).

<sup>21</sup>F. Albert Cotton, *Chemical Applications of Group Theory* (Wiley-Interscience, New York, 1970), p. 266.

<sup>22</sup>Y. Tanabe and S. Sugano, J. Phys. Soc. Jpn. **9**, 753 (1954).